Supporting Information

Reduced graphene oxide composite aerogel prepared by europium-assisting radiation reduction as a broad-spectrum adsorbent for organic pollutants

Peng Zhang[a], Yizhi Chen[a], Hanqin Weng[a,b,], Yusa Muroya[b], Shinichi Yamashita[c,d], Yinhua Zhao[e], Mingzhang Lin[a]*

a. School of Nuclear Science and Technology, University of Science and Technology of China, Hefei, Anhui 230026, China

b. SANKEN (The Institute of Scientific and Industrial Research), Osaka University, 8-1 Mihogaoka, Ibaraki, Osaka 567-0047, Japan

c. Nuclear Professional School, School of Engineering, The University of Tokyo, 2-22 Shirakata-shirane, Tokai-mura, Naka-gun, Ibaraki 319-1188, Japan

d. Department of Nuclear Engineering and Management, School of Engineering, The University of Tokyo, 4-7-1 Hongo, Bunkyo-ku, Tokyo 113-8656, Japan

e. Instruments Center for Physical Science, University of Science and Technology of China, Hefei, Anhui 230026, China

* To whom correspondence should be addressed. Email: hanqinw@ustc.edu.cn (H. Q. Weng)

1. Pulse radiolysis experiments

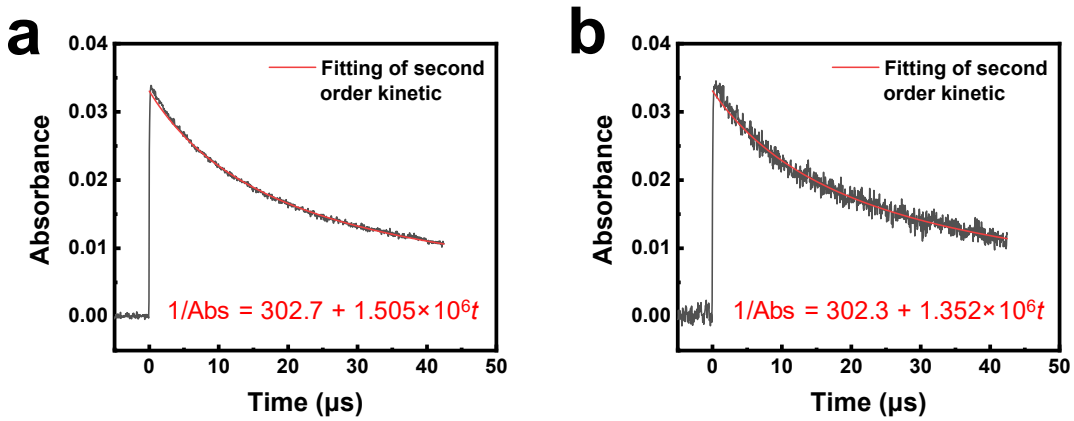

Figure. S1 Decay curves of the absorbance for $(CH_3)_2\dot{C}OH$ at 300 nm in isopropanol (0.2 mol L^{-1}) aqueous solution with (**a**) and without (**b**) the addition of GO (0.15 mg mL^{-1}). The absorbed dose in pulse radiolysis experiments was 65 Gy $pulse^{-1}$.

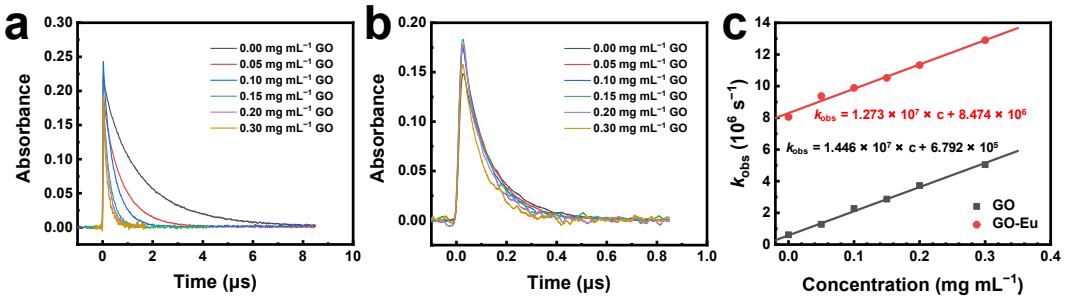

Figure. S2 Decay curves of the absorbance for e_{aq}^- at 720 nm with (**a**) and without 0.13 mmol L^{-1} of Eu^{3+} (**b**). Apparent reaction rates between e_{aq}^- and GO (**c**). The aqueous dispersion contained 0.2 mol L^{-1} of isopropanol and different concentrations of GO. The absorbed dose in pulse radiolysis experiments was 16 Gy $pulse^{-1}$.

The rate constant between e_{aq}^- and GO was calculated as follows.

For a second-order reaction,

$$A + B \rightarrow C \tag{S1}$$

The reaction rate can be expressed as,

$$-\frac{d[A]}{dt} = k[A][B] \tag{S2}$$

where [A] and [B], whose units are both $mol \cdot L^{-1}$, are the concentrations of A and B respectively. k is the rate constant of the second-order reaction, whose unit is $L \cdot mol^{-1} \cdot s^{-1}$. When the concentration of B is much higher than that of A, the concentration of B almost remains constant during the reaction. Thus [A] decays according to a pseudo-first-order reaction kinetics. Then **Equation S2** is simplified to **Equation S3**.

$$-\frac{d[A]}{dt} = k'[B] \tag{S3}$$

where $k' = k$[B]. The unit of k' is s^{-1}.

The apparent reaction rate (k_{obs}) of e_{aq}^- in **Figure. S2c** is the k' in **Equation S3**. The concentration of GO was much higher than that of e_{aq}^- produced by water radiolysis. Thus k between e_{aq}^- and GO was obtained by linear fitting of the k_{obs} *vs.* [GO] plots.

After addition of Eu^{3+}, the linear fitting displayed an intercept of 8×10^6 s^{-1}, which was caused by the rapid reaction between e_{aq}^- and Eu^{3+}. The k between e_{aq}^- and Eu^{3+} was estimated to be 6.5×10^{10} $L\ mol^{-1}\ s^{-1}$ ($8.5 \times 10^6\ s^{-1}/1.3 \times 10^{-4}\ mol\ L^{-1}$).

2. Eu^{3+}-induced pre-assembly of GO

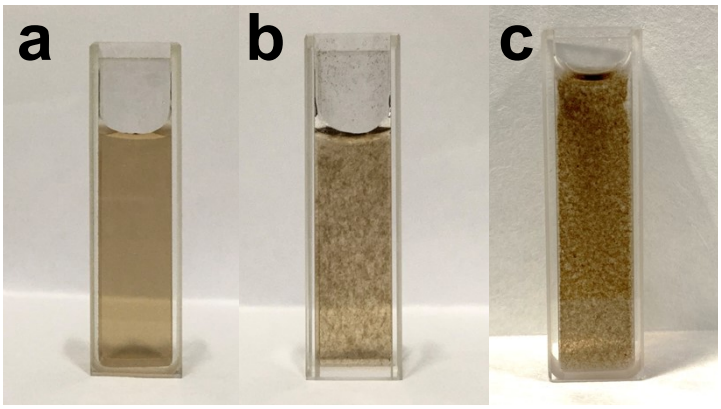

Figure. S3. Photographs of GO dispersion (**a**), GO dispersion with addition of Eu^{3+} at pH 2 (**b**) and 6 (**c**).

3. Characterization of pristine GO

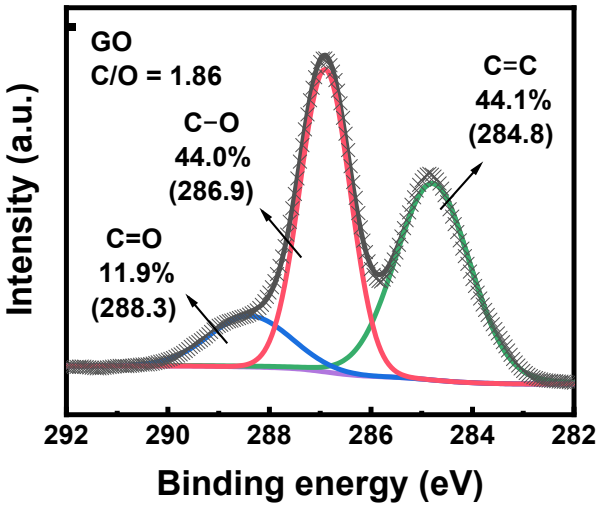

Figure. S4 XPS C 1s spectrum of GO.

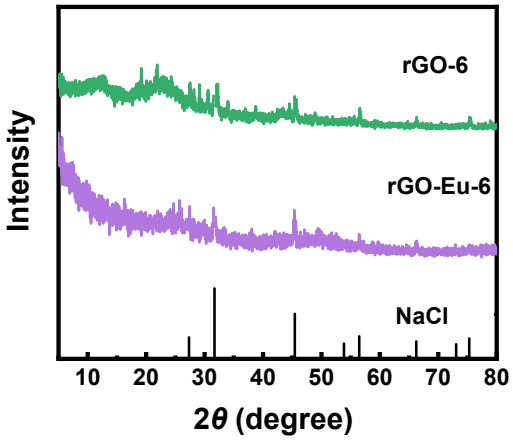

Figure. S5 XRD patterns of rGO-6 and rGO-Eu-6, diffraction peaks of NaCl (JCPDS Card no. 05-0628).

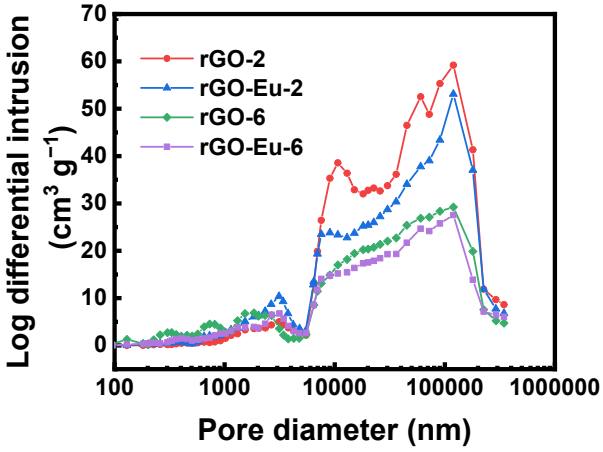

Figure. S6 Pore size distributions of rGO-2, rGO-Eu-2, rGO-6, and rGO-Eu-6 measured by mercury intrusion porosimetry.

4. Comparison in the adsorption performance

Table S1. Comparison in the maximum adsorption capacities (q_m) of organic pollutants on different adsorbents.

Adsorbents	q_m for organic solvents ($g\ g^{-1}$)	q_m for organic dyes ($mg\ g^{-1}$)	Ref.
graphene sponge	20–86	–	[1]
reduced graphene oxide foam	70–122	–	[2]
Freeze-dried CNF/graphene	44–265	–	[3]
CdS/RGO aerogel	122–298	–	[4]
Cyclodextrin/graphene oxide aerogel	–	186.2 (methyl orange)	[5]
Functionalized graphene oxide aerogel	–	202.8 (methyl orange)	[6]
Carbon nanotubes and cellulose nanofiber incorporated graphene aerogel	–	51.6 (methyl orange) 101.0 (rhodamine 6G)	[7]
Cellulose/graphene oxide composite aerogel	–	68 (methylene B)	[8]
Layered double hydroxides-assembled graphene oxide aerogel	–	96–125 (methylene B)	[9]
rGO-Eu-2 aerogel	81–395	1173.4 (eriochrome black T) 230.4 (methyl orange) 906.8 (malachite green) 173.7 (rhodamine 6G) 206.8 (methylene B)	This work
rGO-Eu-6 aerogel	12–25	1572.5 (eriochrome black T) 312.6 (methyl orange) 1367.6 (malachite green) 160.9 (rhodamine 6G) 95.4 (methylene B)	This work

5. Solid-state excitation and emission spectra of rGO-Eu-2

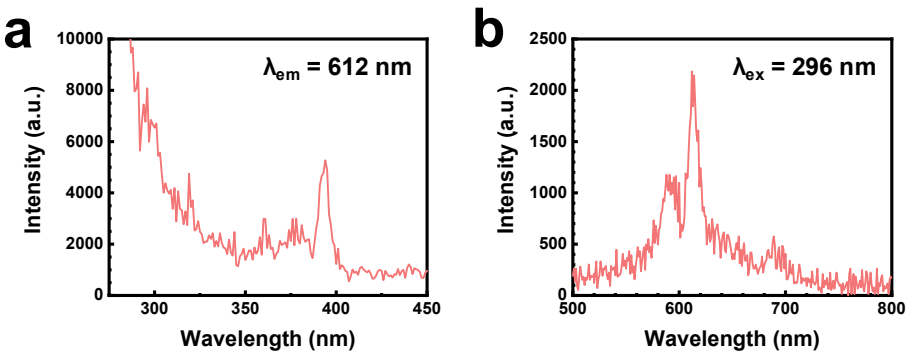

Figure. S7. Solid-state excitation (**a**) and emission (**b**) spectra of rGO-Eu-2.

6. UV-vis absorption spectra of different organic solvents

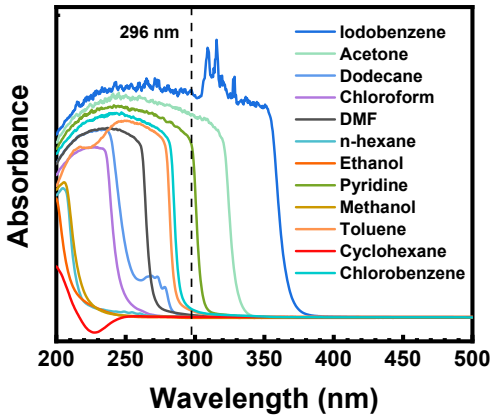

Figure. S8. UV-vis absorption spectra of different organic solvents.

7. Adsorption performance for anionic dyes

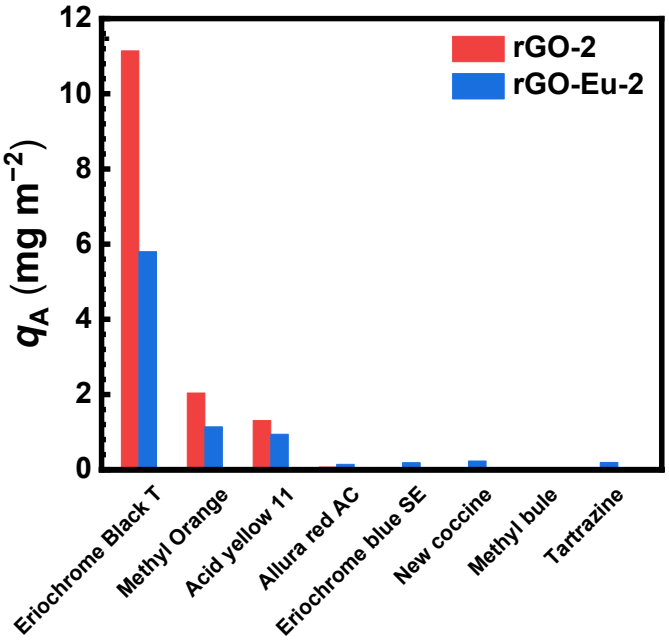

Figure. S9 Adsorption amounts of anionic dyes on per unit area of rGO-2 and rGO-Eu-2 aerogels.

8. Calculation of Eu contents in rGO-Eu aerogels

The contents of Eu in aerogels were obtained according the concentration of Eu in dispersion before and after irradiation. The contents were calculated by the following **Equation S4**,

$$Content = \frac{(c_0 - c_e) \times V}{m} \quad \text{(S4)}$$

where c_0 (mg L^{-1}) and c_e (mg L^{-1}) are the concentrations of Eu in dispersion before and after irradiation, respectively. m (g) and V (L) are the weight of GO and the volume of dispersion, respectively. For determining the concentration of Eu after irradiation (c_e), supernate of irradiated dispersion was obtained by centrifugation (10000 rpm, 5 min). Then Eu concentration of supernate was determined using an inductively coupled plasma optical emission spectrometer (ICP-OES, PerkinElmer Optima 7300DV).

Reference

[1] H. Bi, X. Xie, K. Yin, Y. Zhou, S. Wan, L. He, F. Xu, F. Banhart, L. Sun, R.S. Ruoff, Spongy graphene as a highly efficient and recyclable sorbent for oils and organic solvents, Adv Funct Mater 22(21) (2012) 4421-4425. https://doi.org/10.1002/adfm.201200888.

[2] Y. He, Y. Liu, T. Wu, J. Ma, X. Wang, Q. Gong, W. Kong, F. Xing, Y. Liu, J. Gao, An environmentally friendly method for the fabrication of reduced graphene oxide foam with a super oil absorption capacity, J Hazard Mater 260 (2013) 796-805. https://doi.org/10.1016/j.jhazmat.2013.06.042.

[3] X. Yao, W. Yu, X. Xu, F. Chen, Q. Fu, Amphiphilic, ultralight, and multifunctional graphene/nanofibrillated cellulose aerogel achieved by cation-induced gelation and chemical reduction, Nanoscale 7(9) (2015) 3959-3964. https://doi.org/10.1039/c4nr07402e.

[4] R. Xu, W. Liu, J. Cai, Z. Li, Robust RGO composite aerogels with high adsorption capabilities for organic pollutants in water, Sep Purif Technol 257 (2021) 117876. https://doi.org/10.1016/j.seppur.2020.117876.

[5] Z.-J. Nie, Q.-F. Guo, H. Xia, M.-M. Song, Z.-J. Qiu, S.-T. Fan, Z.-H. Chen, S.-X. Zhang, S. Zhang, B.-J. Li, Cyclodextrin self-assembled graphene oxide aerogel microspheres as broad-spectrum adsorbent for removing dyes and organic micropollutants from water, J Environ Chem Eng 9(2) (2021) 104749.

[6] J. Xu, P. Du, W. Bi, G. Yao, S. Li, H. Liu, Graphene oxide aerogels co-functionalized with polydopamine and polyethylenimine for the adsorption of anionic dyes and organic solvents, Chem Eng Res Des 154 (2020) 192-202.

[7] T. Shimizu, K.K.H. De Silva, M. Hara, M. Yoshimura, Facile synthesis of carbon nanotubes and cellulose nanofiber incorporated graphene aerogels for selective organic dye adsorption, Appl Surf Sci

600 (2022) 154098.

[8] Fang, Ren, Zhen, Li, Wen-Zhen, Tan, Xiao-Hui, Liu, Zhen-Feng, Sun, Facile preparation of 3D regenerated cellulose/graphene oxide composite aerogel with high-efficiency adsorption towards methylene blue, J Colloid Interf Sci (2018) https://doi.org/10.1016/j.jcis.2018.07.101.

[9] Q. Fang, B. Chen, Self-assembly of graphene oxide aerogels by layered double hydroxides cross-linking and their application in water purification, J Mater Chem A 2(23) (2014) 8941-8951. https://doi.org/10.1039/C4TA00321G.